Double ionization of He($1s^2$) and He($1s2s\ ^3S$) by a single high-energy photon

Zhong-jian Teng and Robin Shakeshaft
Physics Department, University of Southern California, Los Angeles, California 90089-0484
(Received 12 November 1993)

We have calculated the energy and angular distributions for double ionization of He($1s^2$) and He($1s2s\ ^3S$) by one photon, over a range of photon energies up to a few keV. The calculations were based on using a fairly accurate initial-state wave function, determined so as to exactly satisfy the Kato cusp conditions, and a final-state wave function which is a product of three Coulomb wave functions modified by a short-range correction term. There are at least three different mechanisms for double ionization, and each one leaves a mark on the angular distribution. When the energies of the two electrons are equal, the contribution of each mechanism to the angular asymmetry parameter can be estimated on theoretical grounds; we compare these estimates with the calculated results to give a further indication of the roles of the various mechanisms. Concerning the shapes of the energy and angular distributions, we find significant differences between double ionization of singlet and triplet helium; in particular, the probability for one high-energy photon to eject two equal-energy electrons from triplet helium nearly vanishes owing to the Pauli exclusion principle and to interference effects resulting from antisymmetrization. In two appendixes we present some details of the integration involved in the calculations.

PACS number(s): 32.80.Fb

I. INTRODUCTION

Recently [1] we reported on calculations of the energy and angular distributions for double ionization of ground-state He by one photon over a range of energies from several hundred eV up to a few keV. Our calculations included electron-electron correlation in both initial *and* final states. We found various structures in the angular distributions, and we associated each structure with one of three different mechanisms for double ionization. In this paper we describe our method in more detail, and we present additional results, not only for ground-state He but also for He initially in the $(1s2s)^3S$ metastable state.

The three mechanisms whereby one photon can eject two electrons are shakeoff, knockout, and photon sharing. (We ignore Rayleigh scattering, which, however, does become important at photon energies above 3 keV or so [2,3].) Each of these mechanisms loosely corresponds to a diagram in a many-body perturbation-theory approach (see, e.g., Refs [4]–[6]). In shakeoff, one electron is shaken out of the atom by the sudden change in the effective nuclear charge that occurs when the other electron absorbs a photon and departs rapidly [7]. Shakeoff involves a "soft" collision between the electrons, prior to the absorption of the photon; were it not for the swift removal of one of the electrons, the equilibrium of the atom would be maintained through further soft collisions between the electrons. Since the collision is *soft*, shakeoff is only effective in producing one slow electron and one fast electron, not two fast electrons. However, two fast electrons can emerge via the knockout mechanism; as in shakeoff, one of the electrons absorbs the photon, but on its way out of the atom, this fast electron undergoes a *hard binary* collision with the other electron [4]–[6], [8]–[10]. Knockout is often referred to as the two-step 1 (TS1) process [6]. In both shakeoff and knockout, the large net momentum carried away by the electrons must originate from a hard collision with the nucleus since the photon can impart energy but not momentum to the electrons (we neglect retardation throughout). However, if the two electrons share the photon, they can both leave with high speed without exchanging as much momentum with the nucleus as in knockout. In fact, almost no net momentum need be exchanged with the nucleus if the two electrons share the photon energy almost equally; for they can leave with nearly (though perhaps not exactly, see below) equal and opposite momenta.

In shakeoff, the screening of the nucleus by one of the electrons plays a crucial role, but the correlation between the electrons plays no role. On the other hand, correlation in the final continuum state plays a crucial role in knockout, and correlation in the initial bound state plays a crucial role in photon sharing. In fact, photon sharing is often referred to simply as bound-state correlation [6]. Proton sharing is somewhat inhibited since two identical charged particles which are otherwise free cannot absorb radiation—their electric dipole depends only on their center-of-mass coordinate, and if there is no external force, the center of mass, and therefore the dipole, does not accelerate, and hence cannot absorb radiation. Consequently, while an isolated electron-positron pair can absorb radiation, two electrons can absorb radiation only in the presence of a third body—in our case, the nucleus. Thus the photon can be shared by the electrons only if they are close to each other *and* to the nucleus. When the initial state is a spin-triplet state, photon sharing is especially inhibited since the Pauli exclusion principle prevents the two electrons from moving close to each other. Even when the initial state is spin singlet, the two electrons cannot emerge with *exactly* equal and opposite

momenta, a rule which, as shown in Sec. II, follows from inversion symmetry. Furthermore, when the initial state is spin triplet, knockout is ineffective in producing two equal-energy electrons; as discussed in Sec. III, this is due to interference effects resulting from antisymmetrization.

As noted above, the different mechanisms leave their mark on the angular distribution. Furthermore, when the energy E_1 of one of the electrons is equal to that of the other, the contribution from each mechanism to the angular asymmetry parameter, $\beta(E_1)$, can be estimated on theoretical grounds. Thus, putting $E_1=E_f/2$, where E_f is the final total energy of both electrons, we show in Sec. II B that $\beta(E_f/2)\approx 1$ if shakeoff is dominant, $\beta(E_f/2)\approx\frac{1}{2}$ if knockout is dominant, and $\beta(E_f/2)\approx -1$ (spin singlet) or 2 (spin triplet) if photon sharing is dominant. A comparison of these estimates with the calculated results reveals further information about the role of each mechanism, at least near the midpoint of the energy distribution.

Of course, it is not always possible to physically distinguish the different mechanisms. In particular, both shakeoff and photon sharing are significant near the boundaries of the energy distribution, where one electron is moving slowly and the other rapidly. In this energy region—which contributes the most to the total cross section—one cannot physically separate photon sharing from shakeoff since so little energy is given up by the photon to the slow electron. The relative contributions of the different mechanisms to the total cross section are gauge invariant only to the extent that these mechanisms can be physically distinguished. Indeed, Dalgarno and Sadeghpour [11] have pointed out that the relative contributions of different diagrams in a many-body perturbation-theory approach are very different in different gauges, while the sum of these contributions is necessarily gauge invariant. This was recently confirmed by Hino *et al.* [12] who calculated the relative contributions of the different diagrams to the total cross section for double ionization of ground-state helium using the length, velocity, and acceleration forms of the photon-atom interaction.

It is well known [13,11] that cross sections for electron ejection by high-energy photons are sensitive to the degree of accuracy to which the initial bound-state wave function satisfies the Kato cusp conditions [14]. In our previous work [1] we determined the bound-state wave function from the minimization of the bound-state energy, without additional constraints; the Kato cusp conditions were satisfied to within a few percent. However, now we determine the bound-state wave function by imposing constraints that guarantee the Kato cusp conditions are satisfied exactly—fortunately, the previous results are not greatly changed. As before, we use a final continuum-state wave function which has the proper asymptotic form, namely, a product of three Coulomb wave functions [15,16], which we modify by the inclusion of a term which partly corrects for the error in the inner region.

In Sec. II we outline the method we used to perform our calculations, and we derive various properties of the asymmetry parameter. In Sec. III we present our results. The integration involved in the calculations is rather arduous, and in Appendixes A and B we describe some aspects of this integration.

II. METHOD

Unless specified otherwise, we use atomic units. We neglect the spin-orbit interaction, and factor out the spin variables from the wave function. The atomic Hamiltonian is

$$H_a=\frac{\mathbf{p}_1^2}{2}+\frac{\mathbf{p}_2^2}{2}-\frac{Z}{r_1}-\frac{Z}{r_2}+\frac{1}{r_3}\ , \tag{1}$$

where $\mathbf{r}_1$ and $\mathbf{r}_2$ are the electron coordinates and $\mathbf{r}_3\equiv\mathbf{r}_2-\mathbf{r}_1$ their relative coordinate, with $r_1=|\mathbf{r}_1|$, $r_2=|\mathbf{r}_2|$, and $r_3=|\mathbf{r}_3|$.

A. Ionization amplitude

We assume that the light is linearly polarized (along the z axis) and we work in the velocity gauge. Let $\mathbf{k}_1$ and $\mathbf{k}_2$ be the final momenta of the two electrons, with $E_1\equiv k_1^2/2$ and $E_2\equiv k_2^2/2$ their final energies. The total final energy is $E_f\equiv E_1+E_2$. The amplitude for double ionization by one photon is

$$f(\mathbf{k}_1,\mathbf{k}_2)=\left\langle \Psi^{(-)}_{\mathbf{k}_1,\mathbf{k}_2}\middle|\left[\frac{d}{dz_1}+\frac{d}{dz_1}\right]\middle|\Psi_i\right\rangle\ , \tag{2}$$

where $|\Psi_i\rangle$ and $|\Psi^{(-)}_{\mathbf{k}_1,\mathbf{k}_2}\rangle$ represent the initial and final states of the atomic system. Let θ_1 and θ_2 be the angles which $\mathbf{k}_1$ and $\mathbf{k}_2$ make with the z axis, and let θ_{12} be the angle between $\mathbf{k}_1$ and $\mathbf{k}_2$. Since the atom absorbs only one unit of angular momentum and is initially in a spherically symmetric state, the ionization amplitude has the form

$$f(\mathbf{k}_1,\mathbf{k}_2)=g(k_1,k_2,\cos\theta_{12})\cos\theta_1 \pm g(k_2,k_1,\cos\theta_{12})\cos\theta_2\ , \tag{3}$$

where $k_1=|\mathbf{k}_1|$ and $k_2=|\mathbf{k}_2|$, where the function $g(k_1,k_2,\cos\theta_{12})$ is to be determined and where the sign is plus (minus) if the atom is initially in a spin-singlet (triplet) state. Note that Eq. (3) implies that if the initial state is spin singlet, we have $f(\mathbf{k},-\mathbf{k})=0$, a consequence of inversion symmetry (and antisymmetrization); hence the two electrons cannot emerge with equal and opposite velocity.

In principle, $g(k_1,k_2,\cos\theta_{12})$ can be calculated by evaluating $f(\mathbf{k}_1,\mathbf{k}_2)$ for $\mathbf{k}_1$ in the xz plane and $\mathbf{k}_2$ along the x axis, so that $\cos\theta_2=0$ and $\cos\theta_1=\sin\theta_{12}$; thus, with reference to the Cartesian system (x,y,z), if we choose

$$\mathbf{k}_1=\mathbf{k}_1'\equiv(\cos\theta_{12},0,\sin\theta_{12})$$

and $\mathbf{k}_2=\mathbf{k}_2'\equiv k_2(1,0,0)$, we have

$$g(k_1,k_2,\cos\theta_{12})=f(\mathbf{k}_1',\mathbf{k}_2')/\sin\theta_{12}\ . \tag{4}$$

However, we found it more expedient to explicitly identify $g(k_1,k_2,\cos\theta_{12})$ as the coefficient of $\cos\theta_1$ in the computed expression for $f(\mathbf{k}_1,\mathbf{k}_2)$.

B. Differential cross section

The differential cross section for the atom to absorb one photon, of frequency ω, and for the two electrons to emerge into solid angles $d\Omega_1$ and $d\Omega_2$ is

$$\frac{d\sigma}{dE_1 d\Omega_1 d\Omega_2}=\frac{4\pi^2}{\omega c}k_1 k_2|f(\mathbf{k}_1,\mathbf{k}_2)|^2 . \quad (5)$$

Integrating the right-hand side of Eq. (5) over all directions of $\mathbf{k}_2$, using Eq. (3), gives the well-known result [17]

$$\frac{d\sigma}{dE_1 d\Omega_1}=\frac{1}{4\pi}\frac{d\sigma}{dE_1}[1+\beta(E_1)P_2(\cos\theta_1)] . \quad (6)$$

The energy distribution $d\sigma/dE_1$ and the angular asymmetry parameter $\beta(E_1)$ can be expressed in terms of the auxiliary functions

$$u(k_1,k_2,l)=\left[\frac{2l+1}{2}\right]\int_{-1}^{1}d\mu|g(k_1,k_2,\mu)|^2P_l(\mu) , \quad (7)$$

$$v(k_1,k_2,l)=2\left[\frac{2l+1}{2}\right]\int_{-1}^{1}d\mu\,\mathrm{Re}[g(k_1,k_2,\mu)\times g^*(k_2,k_1,\mu)]P_l(\mu) . \quad (8)$$

After some algebra we find that

$$\frac{d\sigma}{dE_1}=\frac{64\pi^4 k_1 k_2}{3\omega c}[u(k_1,k_2,0)+u(k_2,k_1,0)\pm\tfrac{1}{3}v(k_1,k_2,1)] , \quad (9)$$

$$\beta(E_1)=\frac{2[15u(k_1,k_2,0)+3u(k_2,k_1,2)\pm 5v(k_1,k_2,1)]}{15[u(k_1,k_2,0)+u(k_2,k_1,0)\pm\frac{1}{3}v(k_1,k_2,1)]} . \quad (10)$$

Note that $v(k_1,k_2,l)$ is symmetric in k_1 and k_2 but that $u(k_1,k_2,l)$ is not. Hence, $d\sigma/dE_1$ is symmetric about the midpoint $E_f/2$, where $E_f\equiv E_1+E_2$, while $\beta(E_1)$ is asymmetric. The reason that $d\sigma/dE_1$ is symmetric about $E_f/2$ is that if one electron emerges with energy E_1, the other electron must emerge with energy E_f-E_1. However, $\beta(E_1)$ is asymmetric because it characterizes an electron of energy E_1 moving in a particular direction; the angles of the other electron, moving with energy E_f-E_1, have been integrated over.

We briefly note here some other properties of the asymmetry parameter. Since

$$-0.5\le P_2(\cos\theta_1)\le 1$$

and since $d\sigma/(dE_1 d\Omega_1)$ is positive, we have

$$-1\le\beta(E_1)\le 2 . \quad (11)$$

If shakeoff were the only mechanism for double ionization, we would need to take into account only the screening of the nucleus by one electron, and not the correlation between the electrons. In this case the initial and final states would each be represented by a (symmetrized or antisymmetrized) product of one-particle wave functions, and $g(k_2,k_1,\mu)$ would be independent of μ, so that $u(k_1,k_2,l)$ and $v(k_1,k_2,l)$ would vanish for $l\neq 0$. Hence, if correlation were weak, we would have

$$\beta(E_1)\approx\frac{2u(k_1,k_2,0)}{u(k_1,k_2,0)+u(k_2,k_1,0)} ,$$

and at the midpoint $E_f/2$, where $k_1=k_2$, we would have

$$\beta(E_f/2)\approx 1 . \quad (12)$$

Thus any departure from $\beta(E_f/2)=1$ is a measure of correlation, albeit only at the midpoint of the energy distribution. Since

$$v(k,k,l)=2u(k,k,l) ,$$

the exact expression for the asymmetry parameter at the midpoint is (with $k^2=E_f$)

$$\beta(E_f/2)=\frac{[15u(k,k,0)+3u(k,k,2)\pm 10u(k,k,1)]}{5[3u(k,k,0)\pm u(k,k,1)]} . \quad (13)$$

If knockout were to dominate, the two electrons would emerge with a relative angle of $\pi/2$ (see Sec. III). To assess the influence of knockout on the value of $\beta(E_f/2)$, we suppose the angular probability distribution to be a Gaussian peaked at $\theta_{12}=\pi/2$, i.e.,

$$|g(k,k,\cos\theta_{12})|^2\propto\exp\left[-\frac{(\cos\theta_{12}-\cos\pi/2)^2}{\sigma_0^2}\right] ;$$

this gives, for both spin-singlet and -triplet states,

$$\beta(E_f/2)\approx\tfrac{1}{2}+\tfrac{3}{4}\sigma_0^2 . \quad (14)$$

If the probability distribution were infinitely sharp ($\sigma_0=0$), we would have $\beta(E_f/2)\approx 1/2$. On the other hand, to assess the influence of photon sharing on the value of $\beta(E_f/2)$, we suppose the angular probability distribution to be a Gaussian peaked at $\theta_{12}=\pi$, i.e.,

$$|g(k,k,\cos\theta_{12})|^2\propto\exp\left[-\frac{(\cos\theta_{12}-\cos\pi)^2}{\sigma_0^2}\right] ;$$

this gives, for the spin-singlet case,

$$\beta(E_f/2)\approx -1+\frac{3\sqrt{\pi}\sigma_0}{4} . \quad (15)$$

and for the spin-triplet case,

$$\beta(E_f/2)\approx 2-\frac{3\sigma_0}{2\sqrt{\pi}} . \quad (16)$$

If the probability distribution were infinitely sharp, we would have $\beta(E_f/2)\approx -1$ for the singlet case, which according to Eq. (6), with $P_2(-1)=1$, implies that the doubly differential cross section vanishes at the midpoint $E_1=E_2=E_f/2$; this is consistent with the fact that, for a spin-singlet state, the triply differential cross section vanishes when $\mathbf{k}_1=-\mathbf{k}_2$. Although the energy region near the double-ionization threshold, where the Wannier mechanism [18] is relevant, is not addressed in this paper, we note that the behavior of the cross section near threshold has been examined [19,20] under the assump-

tion that the two electrons recede along the Wannier ridge with equal energies ($E_f/2$) and in opposite directions, with an angular probability distribution that is Gaussian [21].

C. Initial state

We took the initial-state wave function $\Psi_i(\mathbf{r}_1,\mathbf{r}_2)$ to have the form

$$\Psi_i(\mathbf{r}_1,\mathbf{r}_2)\approx Ce^{-\lambda_1(r_1+r_2)-\lambda_3 r_3}\sum_{i+j+k\le N} c_{ijk}r_1^i r_2^j r_3^k \ .$$

The coefficients satisfy $c_{ijk}=\pm c_{jik}$, where the plus (minus) sign is chosen to guarantee that the wave function is symmetric (antisymmetric). Note, that λ_3 may be positive or negative, as long as $\lambda_1+\lambda_3>0$. The integer N was chosen to be 2 or 3, and the two nonlinear parameters λ_1 and λ_3 and the linear parameters c_{ijk} were chosen to minimize the initial energy E_i of the atom—subject, however, to the constraints of the Kato cusp conditions, which are [14]

$$\left\langle\frac{\partial\Psi_i(\mathbf{r}_1,\mathbf{r}_2)}{\partial r_1}\right\rangle_{r_1=0}=-Z\Psi_i(\mathbf{0}_1,\mathbf{r}_2) \ , \tag{18}$$

$$\left\langle\frac{\partial\Psi_i(\mathbf{r}_1,\mathbf{r}_2)}{\partial r_3}\right\rangle_{r_3=0}=\tfrac{1}{2}\Psi_i(\mathbf{r}_1,\mathbf{r}_2=\mathbf{r}_1) \ , \tag{19}$$

where the average is taken on a sphere of fixed radius—r_1 in Eq. (18) and r_3 in Eq. (19). The first condition pertains to the confluence of one electron and the nucleus, and the second condition pertains to the confluence of the two electrons. The main contribution to the binding energy $|E_i|$ comes from a spatial region whose distance from the nucleus is of the order of the characteristic binding radius, but it is the region much nearer to the nucleus that is most relevant to photoejection. Therefore, the Kato cusp conditions are a more relevant measure [13,11] of the accuracy of $\Psi_i(\mathbf{r}_1,\mathbf{r}_2)$. The number of *free* parameters that can be varied to minimize E_i is reduced by the Kato constraints. As an example of the accuracy of the binding energy $|E_i|$, when the wave functions are constrained to satisfy the Kato cusp conditions, the 8-parameter ($N=2$) and 14-parameter ($N=3$) wave functions yield for He($1s^2$) the energy estimates 2.87 and 2.902, respectively, compared to the highly accurate Pekeris estimate 2.903 724 374 a.u., while for He($1s2s\,^3S$), the 14-parameter ($N=3$) wave function yields the energy estimate 2.14, compared to the highly accurate Pekeris estimate 2.175 229 378 a.u. When the Kato cusp constraints are removed, so all of the parameters are free, considerably more accurate binding energies are obtained [1].

D. Final state

The final-state wave function has the asymptotic form [15,16,22]

$$\chi^{(-)}_{\mathbf{k}_1,\mathbf{k}_2}(\mathbf{r}_1,\mathbf{r}_2)=N(\mathbf{k}_1,\mathbf{k}_2)e^{i\mathbf{k}_1\cdot\mathbf{r}_1+i\mathbf{k}_2\cdot\mathbf{r}_2}\times\prod_{j=1-3}{}_1F_1(i\gamma_j,1,-ik_jr_j-i\mathbf{k}_j\cdot\mathbf{r}_j) \ , \tag{20}$$

where $\mathbf{k}_1+\mathbf{k}_2$ is the momentum of the center of mass of the two electrons, where $\mathbf{k}_3$ is the momentum of the "particle" with reduced mass $\frac{1}{2}$:

$$\mathbf{k}_3=\tfrac{1}{2}(\mathbf{k}_2-\mathbf{k}_1) \ , \tag{21}$$

and where the normalization factor $N(\mathbf{k}_1,\mathbf{k}_2)$ is

$$N(\mathbf{k}_1,\mathbf{k}_2)\equiv\prod_{j=1-3}e^{-\pi\gamma_j/2}\Gamma(1-i\gamma_j) \ , \tag{22}$$

with

$$\gamma_1=-Z/k_1 \ , \tag{23}$$

$$\gamma_2=-Z/k_2 \ , \tag{24}$$

$$\gamma_3=1/(2k_3) \ . \tag{25}$$

Maulbetsch and Briggs [22] and more recently Hino [23] have calculate the double-photoionization cross section using a final-state wave function that is approximated by $\chi^{(-)}_{\mathbf{k}_1,\mathbf{k}_2}(\mathbf{r}_1,\mathbf{r}_2)$. Also, Anderson and Burgdörfer [3] have calculated cross sections for single ionization with simultaneous excitation using a generalization of $\chi^{(-)}_{\mathbf{k}_1,\mathbf{k}_2}(\mathbf{r}_1,\mathbf{r}_2)$ to describe states of He in which one electron is in the continuum while the other is in an excited bound state; by summing over all bound-state probabilities and subtracting from unity, they deduced the ratio of cross sections for double to single photoionization.

One can show that

$$(H_a-E_f)|\chi^{(-)}_{\mathbf{k}_1,\mathbf{k}_2}\rangle=|\phi^{(-)}_{\mathbf{k}_1,\mathbf{k}_2}\rangle \ , \tag{26}$$

where the residual term on the right-hand side is

$$\begin{aligned}\phi^{(-)}_{\mathbf{k}_1,\mathbf{k}_2}(\mathbf{r}_1,\mathbf{r}_2)=&-\frac{Z}{4}N(\mathbf{k}_1,\mathbf{k}_2)e^{i(\mathbf{k}_1\cdot\mathbf{r}_1+\mathbf{k}_2\cdot\mathbf{r}_2)}\,{}_1F_1(1+i\gamma_3,2,-ik_3r_3-i\mathbf{k}_3\cdot\mathbf{r}_3)\\&\times\{{}_1F_1(i\gamma_1,1,-ik_1r_1-i\mathbf{k}_1\cdot\mathbf{r}_1)\,{}_1F_1(1+i\gamma_2,2,-ik_2r_2-i\mathbf{k}_2\cdot\mathbf{r}_2)(\hat{\mathbf{r}}_2+\hat{\mathbf{k}}_2)\cdot(\hat{\mathbf{r}}_3+\hat{\mathbf{k}}_3)\\&+{}_1F_1(i\gamma_2,1,-ik_2r_2-i\mathbf{k}_2\cdot\mathbf{r}_2)\\&\times{}_1F_1(1+i\gamma_1,2,-ik_1r_1-i\mathbf{k}_1\cdot\mathbf{r}_1)(\hat{\mathbf{r}}_1+\hat{\mathbf{k}}_1)\cdot(\hat{\mathbf{r}}_3+\hat{\mathbf{k}}_3)\} \ .\end{aligned} \tag{27}$$

From the asymptotic behavior of the hypergeometric function, i.e.,

$$ {}_1F_1(1+i\gamma_j,2,-ik_jr_j-i\mathbf{k}_j\cdot\mathbf{r}_j) \propto \frac{1}{k_jr_j}\,{}_1F_1(i\gamma_j,1,-ik_jr_j-i\mathbf{k}_j\cdot\mathbf{r}_j) , $$

we have

$$ \phi^{(-)}_{\mathbf{k}_1,\mathbf{k}_2}(\mathbf{r}_1,\mathbf{r}_2) \propto \frac{(\hat{\mathbf{r}}_3+\hat{\mathbf{k}}_3)}{k_3r_3}\left[\frac{(\hat{\mathbf{r}}_1+\hat{\mathbf{k}}_1)}{k_1r_1}+\frac{(\hat{\mathbf{r}}_2+\hat{\mathbf{k}}_2)}{k_2r_2}\right] \times\chi^{(-)}_{\mathbf{k}_1,\mathbf{k}_2}(\mathbf{r}_1,\mathbf{r}_2) , \tag{28} $$

showing that the correction to the asymptotic form falls off as the inverse square of the distance. Note, however, that due to the appearance of the momenta in the denominators on the right-hand side of Eq. (28), the asymptotic form does not become valid until very large distances when any one of these momenta becomes small. Consequently, the asymptotic form becomes less useful as the total final energy E_f decreases. Indeed, the normalization factor $N(\mathbf{k}_1,\mathbf{k}_2)$ is erroneously small when E_f is small; it decreases exponentially as E_f approaches zero.

We write the exact final-state vector $|\Psi^{(-)}_{\mathbf{k}_1,\mathbf{k}_2}\rangle$ as

$$ |\Psi^{(-)}_{\mathbf{k}_1,\mathbf{k}_2}\rangle = |\chi^{(-)}_{\mathbf{k}_1,\mathbf{k}_2}\rangle + |\Phi^{(-)}_{\mathbf{k}_1,\mathbf{k}_2}\rangle , \tag{29} $$

where $|\Phi^{(-)}_{\mathbf{k}_1,\mathbf{k}_2}\rangle$ is the correction to the asymptotic-state vector. Now by combining Eqs. (26) and (29), and requiring that

$$ (H_a-E_f)|\Psi^{(-)}_{\mathbf{k}_1,\mathbf{k}_2}\rangle = 0 , $$

we have

$$ (H_a-E_f)|\Phi^{(-)}_{\mathbf{k}_1,\mathbf{k}_2}\rangle = -|\phi^{(-)}_{\mathbf{k}_1,\mathbf{k}_2}\rangle . \tag{30} $$

We expect the correction $\Phi^{(-)}_{\mathbf{k}_1,\mathbf{k}_2}(\mathbf{r}_1,\mathbf{r}_2)$ to have the form of the plane-wave term

$$ \exp[i(\mathbf{k}_1\cdot\mathbf{r}_1+\mathbf{k}_2\cdot\mathbf{r}_2)] $$

multiplied by a "short"-range function which does not oscillate as rapidly as the plane-wave term. This leads us to expand the short-range factor in terms of the eigenfunctions $\Psi_j(\mathbf{r}_1,\mathbf{r}_2)$ of the atomic Hamiltonian, with

$$ \Psi_0(\mathbf{r}_1,\mathbf{r}_2)=\Psi_i(\mathbf{r}_1,\mathbf{r}_2) . $$

Thus we write

$$ \Phi^{(-)}_{\mathbf{k}_1,\mathbf{k}_2}(\mathbf{r}_1,\mathbf{r}_2) = e^{ib(\mathbf{k}_1\cdot\mathbf{r}_1+\mathbf{k}_2\cdot\mathbf{r}_2)}\sum_j a_j\Psi_j(\mathbf{r}_1,\mathbf{r}_2) , \tag{31} $$

where we have introduced a factor b into the exponent of the plane-wave term in order to retain flexibility, anticipating that the "optimal" value of b will be close to unity. By substituting Eq. (31) into Eq. (30) and denoting the eigenvalues of H_a as E_j (with $E_0=E_i$), we obtain

$$ e^{-ib(\mathbf{k}_1\cdot\mathbf{r}_1+\mathbf{k}_2\cdot\mathbf{r}_2)}\phi^{(-)}_{\mathbf{k}_1,\mathbf{k}_2}(\mathbf{r}_1,\mathbf{r}_2) = \sum_j a_j[E_f(1-b^2)-E_j]\Psi_j(\mathbf{r}_1,\mathbf{r}_2) + ib\sum_j a_j[\mathbf{k}_1\cdot\nabla_1\Psi_j(\mathbf{r}_1,\mathbf{r}_2)+\mathbf{k}_2\cdot\nabla_2\Psi_j(\mathbf{r}_1,\mathbf{r}_2)] . \tag{32} $$

Defining $K\equiv\sqrt{2E_f}$ and

$$ Kd_j(\mathbf{r}_1,\mathbf{r}_2)\equiv i[\mathbf{k}_1\cdot\nabla_1\ln\Psi_j(\mathbf{r}_1,\mathbf{r}_2)+\mathbf{k}_2\cdot\nabla_2\ln\Psi_j(\mathbf{r}_1,\mathbf{r}_2)] , \tag{33} $$

we can rewrite Eq. (32) as

$$ \sum_j a_j[E_f(1-b^2)-E_j+bK\,d_j(\mathbf{r}_1,\mathbf{r}_2)]\Psi_j(\mathbf{r}_1,\mathbf{r}_2) = \phi^{(-)}_{\mathbf{k}_1,\mathbf{k}_2}(\mathbf{r}_1,\mathbf{r}_2)e^{-ib(\mathbf{k}_1\cdot\mathbf{r}_1+\mathbf{k}_2\cdot\mathbf{r}_2)} . \tag{34} $$

For E_f large—the case of interest in this paper—the term $E_f(1-b^2)$ dominates the other terms in the square brackets on the left-hand side of Eq. (34), unless $b\approx1$. Hence, unless we were to choose $b\approx1$, the coefficients a_j in the sum on the left-hand side of Eq. (34) would each be multiplied by roughly the same (large) number, and therefore these coefficients would be of comparable magnitude. Since we need to truncate the sum in practice, we would like to arrange that those coefficients a_j corresponding to eigenfunctions whose eigenvalues E_j lie high up in the continuum are relatively small. To this end, we choose

$$ b=\sqrt{\omega/E_f} ; \tag{35} $$

note that since $E_f=E_i+\omega$, we have $b\approx1$ if $E_f\gg|E_i|$. Consequently, Eq. (34) becomes

$$ \sum_j a_j[\Delta E_{ij}+bK\,d_j(\mathbf{r}_1,\mathbf{r}_2)]\Psi_j(\mathbf{r}_1,\mathbf{r}_2) = \phi^{(-)}_{\mathbf{k}_1,\mathbf{k}_2}(\mathbf{r}_1,\mathbf{r}_2)e^{-ib(\mathbf{k}_1\cdot\mathbf{r}_1+\mathbf{k}_2\cdot\mathbf{r}_2)} , \tag{36} $$

where $\Delta E_{ij}=E_i-E_j$. We expect a_j to be relatively small if E_j is large (since $|\Delta E_{ij}|$ is large). Hence it seems reasonable to truncate the sum. However, we now make a drastic approximation—we truncate the sum to one term only, in order to avoid intractable computation. Thus we approximate Eq. (31) by

$$ \Phi^{(-)}_{\mathbf{k}_1,\mathbf{k}_2}(\mathbf{r}_1,\mathbf{r}_2)\simeq ae^{ib(\mathbf{k}_1\cdot\mathbf{r}_1+\mathbf{k}_2\cdot\mathbf{r}_2)}\Psi_i(\mathbf{r}_1,\mathbf{r}_2) , \tag{37} $$

where b is defined by Eq. (35) and where a is determined by imposing the orthogonality of the final state with the initial state:

$$ a=-\frac{\langle\chi^{(-)}_{\mathbf{k}_1,\mathbf{k}_2}|\Psi_i\rangle}{\langle\Psi_i|\exp[ib(\mathbf{k}_1\cdot\mathbf{r}_1+\mathbf{k}_2\cdot\mathbf{r}_2)]|\Psi_i\rangle} . \tag{38} $$

Hence, we take as the final-state vector

$$ \Psi^{(-)}_{\mathbf{k}_1,\mathbf{k}_2}(\mathbf{r}_1,\mathbf{r}_2)\approx\chi^{(-)}_{\mathbf{k}_1,\mathbf{k}_2}(\mathbf{r}_1,\mathbf{r}_2)+ae^{ib(\mathbf{k}_1\cdot\mathbf{r}_1+\mathbf{k}_2\cdot\mathbf{r}_2)}\Psi_i(\mathbf{r}_1,\mathbf{r}_2) . \tag{39} $$

Despite this rather severe approximation, the comparison of our results with experimental data [27] appears to confirm that the inclusion of the second term on the right-hand side of Eq. (39) does lead to more meaningful results at energies E_f lower than would otherwise have been possible (see Fig. 5 of Ref. [1]). Nevertheless, this correction does not alter the normalization factor and the spurious exponential decrease of the normalization factor means that the estimated absolute cross section will decrease far too rapidly as E_f approaches zero. [Moreover, the parameter b becomes infinite as E_f approaches zero; see Eq. (35).]

III. RESULTS

We begin by showing results for double ionization of ground-state He based on the 8-parameter bound-state wave function and the final-state wave function of Eq. (39). In Fig. 1 we show a slice of the angular distribution, $d\sigma/dE_1 d\Omega_1 d\Omega_2$, in one plane for a photon energy of 2.8 keV. We showed this figure previously [1] but we include it here, and we repeat part of our earlier discussion, for clarification of, and comparison with, our new results. We have fixed the momentum $\mathbf{k}_1$ of one electron—electron 1, say—to be at an angle

$$\theta_1=\cos^{-1}(1/\sqrt{3})=54.73^\circ$$

with the z axis, and we have allowed the momentum $\mathbf{k}_2$ of the other electron—electron 2, say—to vary in the plane of $\mathbf{k}_1$ and the electric field (z) axis. Our choice of θ_1 implies $P_2(\cos\theta_1)=0$, and hence $\int d\Omega_2(d\sigma/dE_1 d\Omega_1 d\Omega_2)$ is, from Eq. (6), the energy distribution $d\sigma/dE_1$ (reduced by $1/4\pi$). We show our slice of the angular distribution versus θ_{12} for four different partitionings of the energy E_f (=2.721 keV). We first focus on the case where one electron carries away almost all the energy, i.e., either E_1 or E_2 equal to 10^{-6} eV. When $E_2=10^{-6}$ eV, we see a peak centered where $\theta_{12}=\pi$. This peak corresponds to shakeoff: Electron 1 absorbs the photon and soars out of the atom, after tickling electron 2. Since electron 2 does not experience the photon, the only direction relevant to this slow electron is the direction of emission of electron 1, and since the electrons repel each other electron 2 prefers to move in the direction opposite to electron 1, i.e., $\theta_{12}=\pi$ is preferred. When $E_1=10^{-6}$ eV, we see two minima and two peaks. The minima, which are almost zeroes, occur at $\theta_{12}=\frac{1}{2}\pi-\theta_1$ and $\theta_{12}=\frac{3}{2}\pi-\theta_1$, corresponding to the unlikely emission of the *fast* electron—now electron 2—perpendicular to the electric-field axis. The fast electron would prefer to emerge along the electric-field axis, i.e., where $\theta_{12}=\pi-\theta_1$ or $\theta_{12}=2\pi-\theta_1$, but in fact the peaks are shifted somewhat closer to π since we have fixed the angle θ_1 of the slow electron, and shakeoff is maximum when $\theta_{12}=\pi$. Now consider the case E_1 or E_2 equal to 50 eV. When $E_2=50$ eV, we see two peaks, one centered close to $\theta_{12}=\pi/2$, the other close to $\theta_{12}=3\pi/2$. While the energy, 50 eV, of the slower electron is not large, it is an appreciable fraction of the initial total binding energy, and the slower electron cannot easily acquire 50 eV via the shakeoff mechanism. Rather, it acquires this energy via the knockout mechanism, and the peaks correspond to the fact that when two particles of equal mass undergo a binary collision, with one of the particles at rest before the collision, they emerge with a relative angle of $\pi/2$ (or $3\pi/2$). When $E_1=50$ eV, the minima once again occur close to where the fast electron emerges perpendicular to the electric field, but now the left and right peaks are shifted somewhat closer to $\pi/2$ and $3\pi/2$, respectively, due to knockout being the more efficient mechanism for ejection

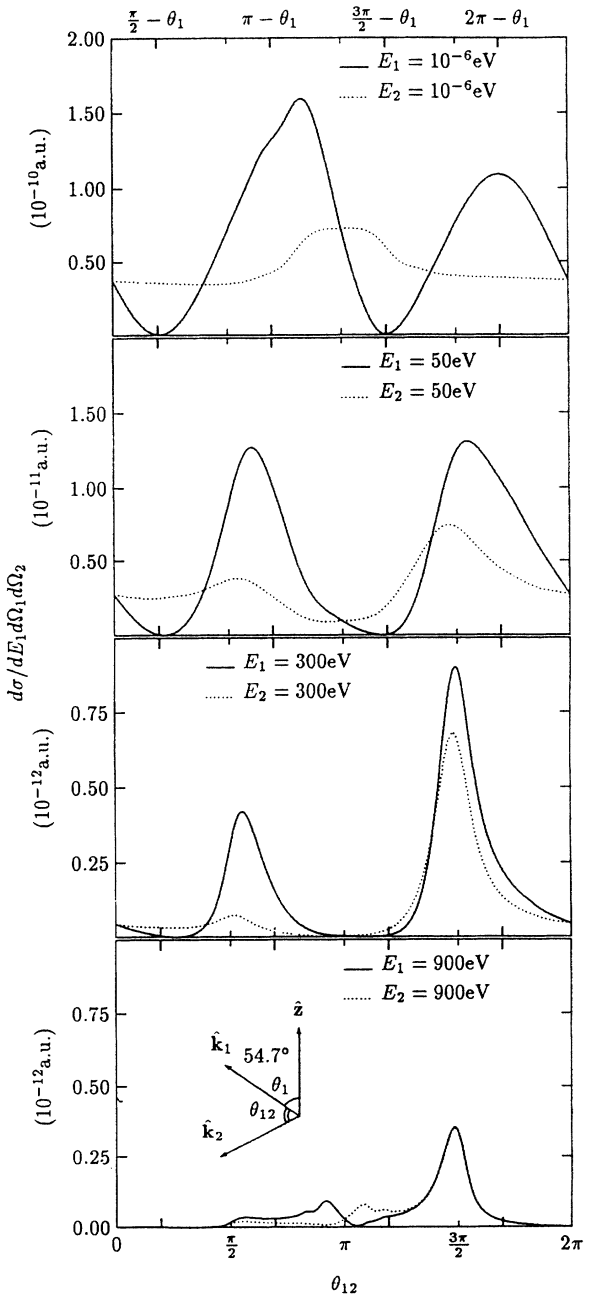

FIG. 1. Angular distribution for double-ionization of He($1s^2$) in the plane formed by the electric field (i.e., the z axis) and the momentum $\mathbf{k}_1$ of one of the electrons, with $\mathbf{k}_1$ fixed at an angle 54.73° with the z axis. The photon energy is 2.8 keV. The thicker tick marks on the θ_{12} axis correspond to values indicated on the upper θ_{12} axis.

of the slower electron (whose angle θ_1 is fixed). Looking now at the case E_1 or E_2 equal to 300 eV, where even the slower electron is moving fast, knockout dominates, and all peaks are centered not far from where $\theta_{12}=\pi/2$ or $3\pi/2$. Note that the peaks near $3\pi/2$ are more pronounced than those near $\pi/2$, a feature which may be understood as follows: The electron which absorbs the photon prefers to be ejected along the electric-field axis, i.e., the positive or negative z axis. Furthermore, this fast electron is deflected through a relatively small angle in the knockout collision. Now, the second electron cannot be knocked out at a large angle (i.e., $>90°$) relative to the direction of incidence of the first electron. Hence, after the knockout collision the two electrons are most likely to emerge within a 90° cone that includes either the negative or, as in our case (since $\theta_1=54.73°$), the positive z axis; therefore, $\theta_{12}=3\pi/2$ is preferred. Finally we consider the case E_1 or E_2 equal to 900 eV, where both electrons are moving very fast and with not very different speeds (note $E_f/2=1360$ eV). Knockout at $\theta_{12}=\pi/2$ is now almost insignificant, while the knockout peaks at $\theta_{12}=3\pi/2$ are almost independent of which electron is fastest. More interestingly, we see a new peak not far from $\theta_{12}=\pi$. This new peak arises from the photon-sharing mechanism, i.e., the two electrons simultaneously share the photon and leave in nearly opposite directions, carrying away almost no net momentum. The minimum close to $\theta_{12}=\pi$ is a vestige of the inversion-symmetry zero of $f(\mathbf{k}_1,\mathbf{k}_2)$ which occurs when $\mathbf{k}_1=-\mathbf{k}_2$.

In Fig. 2 we show the asymmetry parameter $\beta(E_1)$, again for ground-state He, for two different photon energies, 625 eV and 2.8 keV. We see that when E_1 is small, $\beta(E_1)$ is very small. This can be understood after recalling that the slow electron 1 is produced by shakeoff, and it "falls" out of the zero-angular-momentum component of $\Psi_i(\mathbf{r}_1,\mathbf{r}_2)$ without any change in angular momentum; electron 1 therefore emerges nearly isotropically if it is not detected with reference to the fast electron 2, and hence $\beta(E_1)\approx 0$ for $E_1\approx 0$. As E_1 increases, $\beta(E_1)$ becomes negative and remains negative as long as E_1 remains well below E_2. Over this range the slower electron 1 is moving too fast to be produced by shakeoff, and is instead produced primarily by knockout; electron 1 therefore emerges nearly perpendicularly to the fast electron 2. To understand why $\beta(E_1)$ is negative, we first note that immediately after absorbing the photon, the fast electron 2 most likely moves along a direction close to the electric-field axis, and as long as it does not give up a lot of energy during the knockout collision, it will not be deflected far from this axis. In this case electron 1 will most likely emerge nearly perpendicularly to the electric-field axis. Inserting

$$P_2(\cos\theta_1)=(3\cos^2\theta_1-1)/2$$

into Eq. (6) gives

$$d\sigma/(dE_1 d\Omega_1)\propto 1+\beta(E_1)[3\cos(2\theta_1)+1]/4\ .$$

Since

$$1+\beta(E_1)[3\cos(2\theta_1)+1]/4$$

varies from $1+\beta(E_1)$ at $\theta_1=0$ to $1-\beta(E_1)/2$ at $\theta_1=\pi/2$, our bias towards $\theta_1=\pi/2$ implies that a large negative value of $\beta(E_1)$ is favored (but note that the largest negative value allowed is -1) Turning now to the region where E_1 approaches E_2, i.e., the region of the midpoint $E_f/2$, we see that $\beta(E_1)$ becomes positive and remains positive for all higher energies. Recall that at the midpoint the asymmetry parameter would be unity if correlation were negligible, but evidently $\beta(E_f/2)$ is significantly different from unity. In Sec. II B we argued that if knockout were to dominate, we would have $\beta(E_f/2)\approx\frac{1}{2}$, while if photon sharing were to dominate, we would have $\beta(E_f/2)\approx -1$. Since knockout contributes significantly more than photon sharing in the region of the midpoint, it is reasonable to expect $\beta(E_f/2)$ to be slightly less than $\frac{1}{2}$, which appears to be true in Fig. 2. At energies well above the midpoint, $\beta(E_1)$ becomes more positive, and in fact we see that $\beta(E_1)$ approaches 2 as E_1 approaches E_f, which can be understood as follows [22,1]: Electron 1 absorbs the photon from the zero-angular-momentum component of $\Psi_i(\mathbf{r}_1,\mathbf{r}_2)$, and therefore acquires one unit of angular momentum. Since $E_1\gg E_2$, the collision with electron 2 hardly disturbs electron 1, and hence electron 1 emerges with a $\cos^2(\theta_1)$ angular distribution (if it is not detected with reference to electron 2), which requires that $\beta(E_f)\approx 2$.

We now examine the relative importance of the different mechanisms for double ionization of ground-state He. To assess the importance of knockout, we note that this mechanism involves strong electron-electron correlation in the final state. Hence, knockout cannot be described by a final-state wave function that is simply a product of two Coulomb wave functions (that would represent the two electrons moving independently in the presence of a single center of force). Therefore, by approximating the final-state wave function as

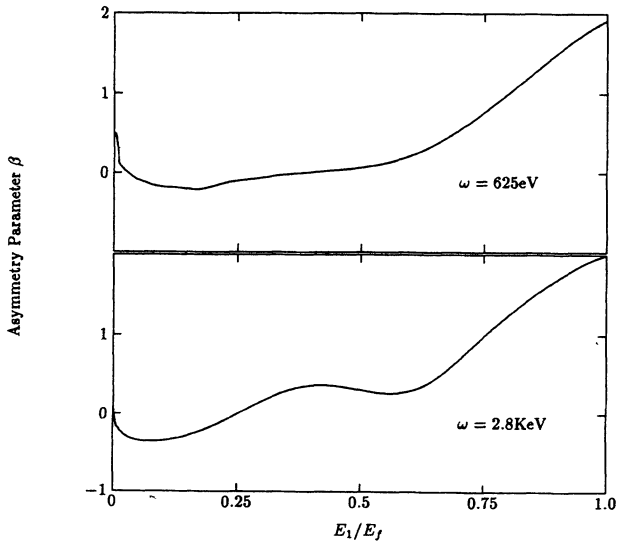

FIG. 2. Asymmetry parameter for double ionization of He($1s^2$) at photon energies of 625 eV and 2.8 keV.

$$\Psi^{(-)}_{\mathbf{k}_1,\mathbf{k}_2}(\mathbf{r}_1,\mathbf{r}_2)\approx(1/2\pi)^3 e^{i\mathbf{k}_1\cdot\mathbf{r}_1+i\mathbf{k}_2\cdot\mathbf{r}_2} \times\prod_{j=1-2} e^{-\pi\alpha_j/2}\Gamma(1-i\alpha_j) \times{}_1F_1(i\alpha_j,1,-ik_jr_j-i\mathbf{k}_j\cdot\mathbf{r}_j)\ , \tag{40}$$

we *exclude* knockout. While a wave function of this form does not explicitly incorporate the electron-electron interaction in the final state, it does so implicitly if we choose $\alpha_1=-Z/k_1$ and $\alpha_2=-(Z-1)/k_1$, thereby taking into account the screening of the nucleus by the slow electron 1 from the fast electron 2. We attribute the cross section calculated by using the final-state wave function of Eq. (40), with full screening by the slow electron, to shakeoff and photon sharing. We can exclude both knockout and photon sharing by ignoring electron-electron correlation in *both* the final *and* initial states. The ground-state wave function

$$\Psi_i(\mathbf{r}_1,\mathbf{r}_2)\approx(Z_{\text{eff}}^3/\pi)e^{-Z_{\text{eff}}(r_1+r_2)}\ , \tag{41}$$

with $Z_{\text{eff}}=\frac{27}{16}$, takes screening but not correlation into account. In Fig. 3 we show three different estimates of the energy distribution $d\sigma/dE_1$ versus E_1, for the two photon energies 625 eV and 2.8 keV. (Since the energy distribution is symmetric about the midpoint $E_f/2$, we show only the half for $E_1\le E_f/2$.) One estimate is based on using the "exact" 8-parameter initial-state wave function and a final-state wave function that is $\chi^{(-)}_{\mathbf{k}_1,\mathbf{k}_2}(\mathbf{r}_1,\mathbf{r}_2)$ of Eq. (20); correlation is included in both initial and final states. A second estimate is based on using the same 8-parameter initial-state wave function and the final-state wave function of Eq. (40); correlation is included in the initial state but not in the final state. A third estimate is based on using the initial-state wave function of Eq. (41) and the final-state wave function of Eq. (40); correlation is not included in either the initial state or final state. The first estimate includes the contributions from shakeoff, knockout, and photon sharing; the second estimate excludes knockout; and the third estimate includes only shakeoff. Integrating the results of Fig. 3 over E_1, we find that shakeoff contributes only about 30% (even less at lower photon energies) of the total double-ionization cross section integrated over energy and angles; this is in accordance with the statements of others [7,11]. Knockout contributes *roughly* 10% or 20%, depending on the photon energy. Of course, we must emphasize again that the relative contributions of the different mechanisms are gauge invariant only to the extent that these mechanisms can be physically distinguished. However, as we see from Fig. 1, it is often not possible to distinguish the different mechanisms unambiguously, and in particular photon sharing is only clearly delineated when both electrons are moving very fast—by the peak in the angular distribution for θ_{12} near π [24].

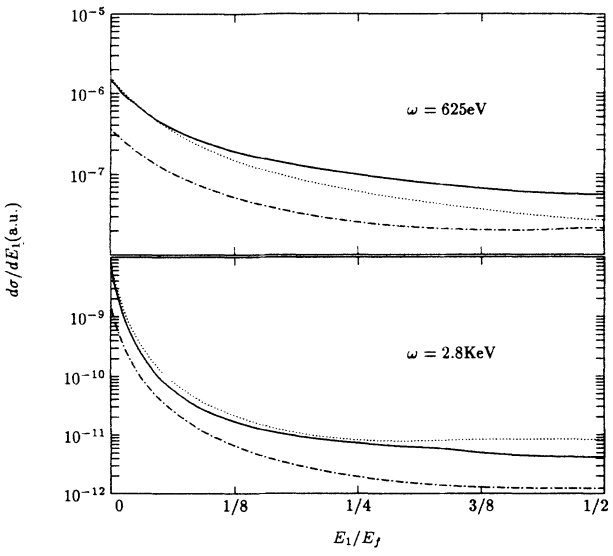

FIG. 3. Estimates of the energy distribution for double ionization of He($1s^2$) at photon energies of 625 eV and 2.8 keV, in three different approximations: solid line, correlation in initial and final states; dotted line, correlation in initial state only; dot-dashed line, no correlation, in either the initial or final state.

We have recalculated the ratio of the cross sections for double and single ionization from ground-state helium by a photon of energy 2.8 keV. To calculate the single-ionization cross section, we multiplied the theoretical results of Ishihara, Hino, and McGuire [6] by a factor which takes into account the contribution from simultaneous excitation; this factor was chosen so as to match the measured data of Samson [25,26] at a photon energy of 450 eV. Using 8- and 14-parameter ground-state wave functions, constrained to satisfy the Kato cusp conditions, and using the final-state wave function of Eq. (39), we calculated the ratio of double- and single-ionization cross sections at 2.8 keV to be 1.53% (8 parameter) and 1.78% (14 parameter), in reasonable agreement with other theoretical results [27,8,13,5,6,11,3,12,23] and with the measured [28] result, 1.6%. We note again that at higher photon energies (above about 3 keV), Rayleigh scattering becomes an important mechanism for both single- and double-ionization [2,3].

We now turn to double ionization of He in the metastable $1s2s\ ^3S$ state. All of our results are based on the 8-parameter bound-state wave function and the final-state wave function of Eq. (39). In Fig. 4 we show a slice of the angular distribution for the same geometry as in Fig. 1 but for a photon energy of 2.0 keV. For $E_1=10^{-6}$ eV, the angular distribution is symmetric about π in θ_{12}, as it should be if shakeoff prevails, but, in contrast to Fig. 1, the angular distribution is suppressed (somewhat) in the neighborhood of π. For $E_1=50$ eV, and also for $E_2=50$ eV, there are, in contrast to Fig. 1, additional minima. We do not know the sources of these differences, but apparently interference effects arise, perhaps due to the different ($1s$ and $2s$) orbits in which the two initially bound electrons move, or to the antisymmetrization of the wave function. For higher energies, e.g., E_1 equal to 300 eV, knockout peaks clearly develop, as in Fig. 1. However, at still higher values of E_1 we do not see a photon-sharing peak developing at θ_{12} near $\pi/2$, and yet, since the joint state is spin triplet, spatial symmetries do

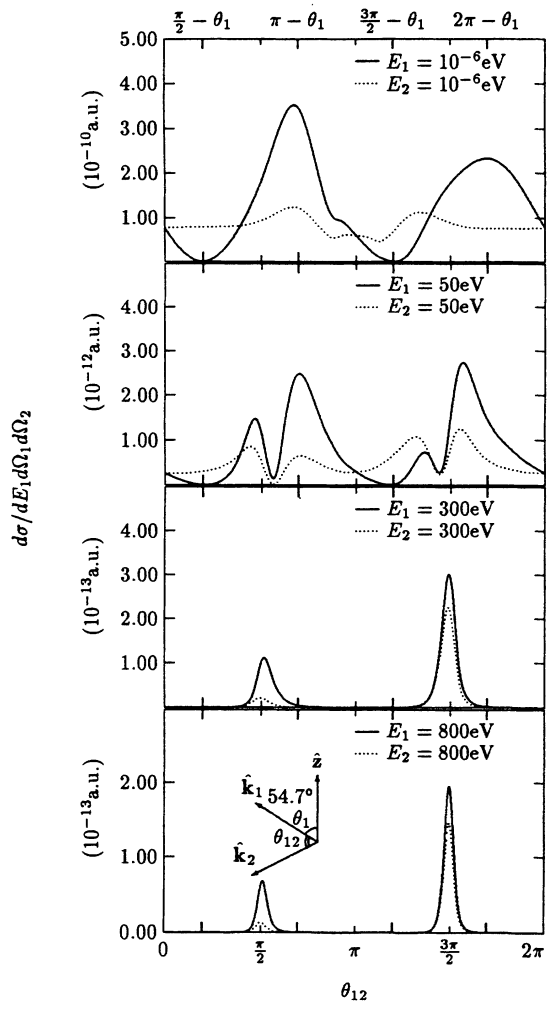

FIG. 4. Angular distribution for double ionization of He($1s2s\ ^3S$) for the same geometry as in Fig. 1. The photon energy is 2.0 keV.

not preclude the two electrons from emerging with equal and opposite velocities (in contrast to double ionization of ground-state helium). In fact, photon sharing is strongly suppressed by the Pauli exclusion principle, which prevents the two electrons from moving close together in a triplet state; only if the two electrons are very close can they share, in comparable proportions, a high-energy photon. In other words, knockout is easily the dominant mechanism in producing two fast electrons in a triplet state (except when the electrons have equal speeds; see below). Of course, photon sharing is still an effective mechanism in producing one slow and one fast electron, since in that case the photon need hardly be shared at all.

In Fig. 5 we show the energy distribution for double ionization of He in the metastable state, for a photon energy of 2.0 keV. The salient difference from Fig. 3 is that the energy distribution dips near the midpoint energy $E_f/2$. (Again, we only show half the energy distribution, in the range $E_1 \leq E_f/2$.) Although not seen in Fig. 4, knockout is strongly suppressed when $E_1 = E_2 (= E_f/2)$, since if two fermions are in a triplet state, and one is initially at rest, the cross section for a collision to result in the two fermions emerging with equal energies vanishes due to the destructive interference resulting from antisymmetrization [29]. Therefore, since shakeoff is ineffective in producing two fast electrons, and since photon sharing is strongly suppressed, the cross section for producing two electrons of equal energies is extremely small; this is why the energy distribution dips near the midpoint.

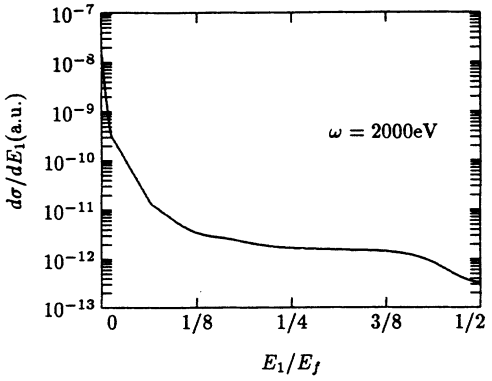

FIG. 5. Energy distribution for double ionization of He($1s2s\ ^3S$) by a photon of energy 2.0 keV.

In Fig. 6 we show the asymmetry parameter for double ionization of metastable He by a photon of energy 2.0 keV. As in Fig. 2, and for the same reasons, $\beta(E_1)$ is very small when E_1 is small, it is negative for E_1 well below E_2, and it is close to 2 when E_1 is near its maximum value E_f. However, we see that $\beta(E_1)$ varies very rapidly when E_1 is in the neighborhood of the midpoint $E_f/2$. This rapid variation is presumably due to the vanishing of the knockout contribution (due to the interference discussed in the preceding paragraph) at the midpoint. At the midpoint, photon sharing, while a weak mechanism, provides the only significant contribution, and as argued in Sec. II B, we have $\beta(E_f/2) \approx 2$ (for spin-triplet states) when photon sharing is dominant. Not too far from the midpoint, we expect $\beta(E_1) \approx \frac{1}{2}$, to the extent that knockout dominates.

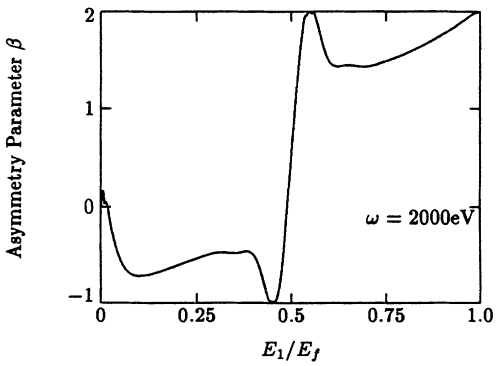

FIG. 6. Asymmetry parameter for double ionization of He($1s2s\ ^3S$) by a photon of energy 2.0 keV.

ACKNOWLEDGMENTS

This work was supported by the Division of Chemical Sciences, Office of Basic Energy Sciences, Office of Energy Research, Department of Energy.

APPENDIX A: REDUCTION OF INTEGRAL

Substitution of the asymptotic wave function, from Eq. (20), into Eq. (2), gives the ionization amplitude $\hat{\mathbf{z}}\cdot\mathbf{A}_0$, where

$$\mathbf{A}_0=\langle\chi^{(-)}_{\mathbf{k}_1,\mathbf{k}_2}(\mathbf{r}_1,\mathbf{r}_2)|i(\nabla_1+\nabla_2)|\Psi_0(\mathbf{r}_1,\mathbf{r}_2)\rangle\ . \tag{A1}$$

When we include the correction to the asymptotic wave function, i.e., Eq. (39), we obtain the amplitude $\hat{\mathbf{z}}\cdot\mathbf{A}$, where

$$\mathbf{A}=\left\langle\chi^{(-)}_{\mathbf{k}_1,\mathbf{k}_2}(\mathbf{r}_1,\mathbf{r}_2)\left|i(\nabla_1+\nabla_2)+\frac{b}{2}(\mathbf{k}_1+\mathbf{k}_2)\right|\Psi_0(\mathbf{r}_1,\mathbf{r}_2)\right\rangle\ . \tag{A2}$$

We define a utility function $U(\lambda_1,\lambda_2,\lambda_3;\mathbf{p}_1,\mathbf{p}_2)$ as

$$U(\lambda_1,\lambda_2,\lambda_3;\mathbf{p}_1,\mathbf{p}_2)=\int\frac{d^3\mathbf{r}_1}{r_1}\int\frac{d^3\mathbf{r}_2}{r_2}\,{}_1F_1(i\gamma_1,1,-ik_1r_1-i\mathbf{k}_1\cdot\mathbf{r}_1)\,{}_1F_1(i\gamma_2,1,-ik_2r_2-i\mathbf{k}_2\cdot\mathbf{r}_2)\,{}_1F_1(i\gamma_3,1,-ik_3r_3-i\mathbf{k}_3\cdot\mathbf{r}_3)$$
$$\times\exp[i(\mathbf{p}_1\cdot\mathbf{r}_1+\mathbf{p}_2\cdot\mathbf{r}_2)-\lambda_1r_1-\lambda_2r_2-\lambda_3r_3] \tag{A3}$$

and express the amplitudes as

$$\mathbf{A}_0=-N(\mathbf{k}_1,\mathbf{k}_2)\sum_{i+j+k\le N}c(i,j,k)\left[-\frac{\partial}{\partial\lambda_3}\right]^k$$
$$\times\left\{\left[-\lambda_1\left[-\frac{\partial}{\partial\lambda_1}\right]^i+i\left[-\frac{\partial}{\partial\lambda_1}\right]^{i-1}\right]\left[-\frac{\partial}{\partial\lambda_2}\right]^{j+1}\nabla_{\mathbf{p}_1}\right.$$
$$\left.+\left[-\lambda_2\left[-\frac{\partial}{\partial\lambda_2}\right]^j+j\left[-\frac{\partial}{\partial\lambda_2}\right]^{j-1}\right]\left[-\frac{\partial}{\partial\lambda_1}\right]^{i+1}\nabla_{\mathbf{p}_2}\right\}$$
$$\times U(\lambda_1,\lambda_2,\lambda_3;\mathbf{p}_1,\mathbf{p}_2)|_{\mathbf{p}_1\to\mathbf{k}_1,\mathbf{p}_2\to\mathbf{k}_2,\lambda_1\to\rho,\lambda_2\to\rho,\lambda_3\to\rho_3} \tag{A4}$$

and

$$\mathbf{A}=\mathbf{A}_0+\frac{b}{2}(\mathbf{k}_1+\mathbf{k}_2)N(\mathbf{k}_1,\mathbf{k}_2)\sum_{i+j+k\le N}c(i,j,k)\left[-\frac{\partial}{\partial\lambda_1}\right]^{i+1}\left[-\frac{\partial}{\partial\lambda_2}\right]^{j+1}\left[-\frac{\partial}{\partial\lambda_3}\right]^k$$
$$\times U(\lambda_1,\lambda_2,\lambda_3;\mathbf{p}_1,\mathbf{p}_2)|_{\mathbf{p}_1\to\mathbf{k}_1,\mathbf{p}_2\to\mathbf{k}_2,\lambda_1\to\rho,\lambda_2\to\rho,\lambda_3\to\rho_3}\ . \tag{A5}$$

Following, Brauner, Briggs, and Klar [15], we can reduce the six-dimensional integral $U(\lambda_1,\lambda_2,\lambda_3;\mathbf{p}_1,\mathbf{p}_2)$ to a two-dimensional integral. During the course of this reduction, we encounter the Lewis three-denominator integral, which we discuss in Appendix B.

APPENDIX B: LEWIS INTEGRAL

In this appendix we reanalyze the Lewis three-denominator integral. The original derivation of the integral can be found in Lewis's paper [30], where the application is to a case when all parameters are real. For a general application when, as in our case, the parameters are complex, we need to choose the integration contour judiciously.

The three-denominator integral is defined as

$$I(\mu_0,\mu_1,\mu_2;\mathbf{q}_0,\mathbf{q}_1,\mathbf{q}_2)=\int\frac{d^3\mathbf{q}}{(\mathbf{q}-\mathbf{q}_0)^2+\mu_0^2}\frac{1}{(\mathbf{q}-\mathbf{q}_1)^2+\mu_1^2}\frac{1}{(\mathbf{q}-\mathbf{q}_2)^2+\mu_2^2}\ , \tag{B1}$$

where the parameters μ_i $(i=0,1,2)$ are, in general, complex, while the $\mathbf{q}_i$'s $(i=0,1,2)$ are real vectors. Note that the integrand of Eq. (B1) is undefined when any of the μ_i is pure imaginary, and therefore the integral representation of

$$I(\mu_0,\mu_1,\mu_2;\mathbf{q}_0,\mathbf{q}_1,\mathbf{q}_2)$$

is valid only for the μ_i in one half-plane. We define

$$I(\mu_0,\mu_1,\mu_2;\mathbf{q}_0,\mathbf{q}_1,\mathbf{q}_2)$$

by the integral representation when the μ_i's have positive real parts, i.e., when the μ_i's are in the right-hand half-plane, and when any μ_i is in the left-hand half-plane, we obtain

$$I(\mu_0,\mu_1,\mu_2;\mathbf{q}_0,\mathbf{q}_1,\mathbf{q}_2)$$

by analytic continuation. Although the integrand is even in each of the μ_i's, this does not imply that

$$I(\mu_0,\mu_1,\mu_2;\mathbf{q}_0,\mathbf{q}_1,\mathbf{q}_2)$$

is an even function of the μ_i's. A simple illustration of this is given by the function π/μ, which is odd in μ but has the integral representation

$$\frac{\pi}{\mu}=\int_{-\infty}^{\infty}\frac{dq}{q^2+\mu^2}\ ; \tag{B2}$$

note that the integrand is undefined for μ on the imaginary axis, but π/μ is analytic for all μ, with a pole at $\mu=0$. However, as Lewis observed,

$$I(\mu_0,\mu_1,\mu_2;\mathbf{q}_0,\mathbf{q}_1,\mathbf{q}_2)$$

does have the following symmetries.

(1) Symmetry by translation. Any translation of the $\mathbf{q}_i$'s simultaneously by a vector $\mathbf{Q}$ preserves the value of

$$I(\mu_0,\mu_1,\mu_2;\mathbf{q}_0,\mathbf{q}_1,\mathbf{q}_2)\ .$$

(2) Symmetry by permutation. Any permutation among the pairs $(\mu_0,\mathbf{q}_0)$, $(\mu_1,\mathbf{q}_1)$, and $(\mu_2,\mathbf{q}_2)$ preserves the value of

$$I(\mu_0,\mu_1,\mu_2;\mathbf{q}_0,\mathbf{q}_1,\mathbf{q}_2)\ .$$

Following Lewis, we convert $I(\mu_0,\mu_1,\mu_2;\mathbf{q}_0,\mathbf{q}_1,\mathbf{q}_2)$ into a one-dimensional integral via a series of fractional transformations. We first derive a special contour in the case where $\mathbf{q}_0=\mathbf{0}$. Using the translation symmetry, we then generalize the contour for arbitrary $\mathbf{q}_0$. Finally, using the permutation symmetry, we generalize to a full range of equivalent contours.

We begin by setting $\mathbf{q}_0=\mathbf{0}$:

$$I(\mu_0,\mu_1,\mu_2;\mathbf{0},\mathbf{q}_1,\mathbf{q}_2)=\int\frac{d^3\mathbf{q}}{q^2+\mu_0^2}\frac{1}{(\mathbf{q}-\mathbf{q}_1)^2+\mu_1^2}\frac{1}{(\mathbf{q}-\mathbf{q}_2)^2+\mu_2^2}\ , \tag{B3}$$

where $\mathrm{Re}(\mu_0,\mu_1,\mu_2)>0$. By the following identity

$$\frac{1}{ab}=\int_0^1\frac{dx}{[ax+b(1-x)]^2}\ , \tag{B4}$$

we obtain

$$\frac{1}{(\mathbf{q}-\mathbf{q}_1)^2+\mu_1^2}\frac{1}{(\mathbf{q}-\mathbf{q}_2)^2+\mu_2^2}=\int_0^1\frac{dx}{[(\mathbf{q}-\mathbf{Q})^2+\Delta^2]^2}\ , \tag{B5}$$

with

$$\mathbf{Q}=x\mathbf{q}_1+(1-x)\mathbf{q}_2\ ,$$
$$\Delta^2=x(1-x)(\mathbf{q}_1-\mathbf{q}_2)^2+x\mu_1^2+(1-x)\mu_2^2\ ,$$
$$\arg(\mu_1,\mu_2)\le\pi/2\ .$$

It follows that

$$\begin{aligned}I(\mu_0,\mu_1,\mu_2;\mathbf{0},\mathbf{q}_1,\mathbf{q}_2)&=\int_0^1dx\int\frac{d^3\mathbf{q}}{\mathbf{q}^2+\mu_0^2}\frac{1}{[(\mathbf{q}-\mathbf{Q})^2+\Delta^2]^2}=\int_0^1dx\int_0^\infty\frac{q^2dq}{q^2+\mu_0^2}\int_{-1}^1\frac{2\pi d\cos\theta}{(q^2+Q^2-2qQ\cos\theta+\Delta^2)^2}\\&=\int_0^1\frac{dx}{Q}\int_{-\infty}^{\infty}\frac{q\,dq}{q^2+\mu_0^2}\frac{\pi}{(q-Q)^2+\Delta^2}\\&=\int_0^1\frac{dx}{\Delta}\frac{\pi^2}{\mu_0^2+x(\mathbf{q}_1^2+\mu_1^2)+(1-x)(\mathbf{q}_2^2+\mu_2^2)+2\Delta\mu_0}\ ,\end{aligned} \tag{B6}$$

with $\mathrm{Re}(\mu_0,\Delta)>0$.

Now we use the following three-step fractional transformation [30]:

$$z=\frac{\mu_1}{\mu_2}\frac{x}{1-x}\ ,$$
$$u=\sqrt{z_1}\left[\frac{z+z_2}{z+z_1}\right]^{1/2}\ ,$$
$$t=\frac{\mathbf{q}_2^2+(\mu_0+\mu_2)^2}{\mu_2(\sqrt{z_1}+\sqrt{z_2})}\sqrt{z_2}\frac{\sqrt{z_1}-u}{u-\sqrt{z_2}}\ ,$$

where

$$\begin{aligned}z_1&=\frac{1}{2\mu_1\mu_2}\{(\mathbf{q}_1-\mathbf{q}_2)^2+\mu_1^2+\mu_2^2\\&\quad-\{[(\mathbf{q}_1-\mathbf{q}_2)^2+\mu_1^2+\mu_2^2]^2-4\mu_1^2\mu_2^2\}\ ,\\z_2&=\frac{1}{z_1}\ .\end{aligned} \tag{B7}$$

After this transformation, we obtain

$$I(\mu_0,\mu_1,\mu_2;\mathbf{0},\mathbf{q}_1,\mathbf{q}_2)=2\pi^2\int_{\xi_t}\frac{dt}{a_0t^2+2b_0t+c_0}\ , \tag{B8}$$

where ξ_t is a contour along $(0,\infty)e^{i\phi_t}$ and

$$\begin{aligned}a_0&=(\mathbf{q}_1-\mathbf{q}_2)^2+(\mu_1+\mu_2)^2\ ,\\b_0&=\mu_0[(\mathbf{q}_1-\mathbf{q}_2)^2+(\mu_1+\mu_2)^2]\\&\quad+\mu_1(\mathbf{q}_2^2+\mu_0^2+\mu_2^2)+\mu_2(\mathbf{q}_1^2+\mu_0^2+\mu_1^2)\ ,\\c_0&=[\mathbf{q}_1^2+(\mu_0+\mu_1)^2][\mathbf{q}_2^2+(\mu_0+\mu_2)^2]\ .\end{aligned} \tag{B9}$$

The angle of the contour ξ_t is

$$\phi_t=\arg\left[\frac{\mu_2[\mathbf{q}_2^2+(\mu_0+\mu_2)^2]}{(\mathbf{q}_1-\mathbf{q}_2)^2+(\mu_1+\mu_2)^2}\right]\ . \tag{B10}$$

We obtain

$$I(\mu_0,\mu_1,\mu_2;\mathbf{q}_0,\mathbf{q}_1,\mathbf{q}_2)$$

from translational symmetry:

$$I(\mu_0,\mu_1,\mu_2;\mathbf{q}_0,\mathbf{q}_1,\mathbf{q}_2)=I(\mu_0,\mu_1,\mu_2;\mathbf{0},\mathbf{q}_1-\mathbf{q}_0,\mathbf{q}_2-\mathbf{q}_0)$$

$$=2\pi^2\int_{\epsilon_v}\frac{dv}{acv^2+2bv+1}\ , \tag{B11}$$

where, introducing

$$m(i,j)=(\mathbf{q}_i-\mathbf{q}_j)^2+(\mu_i+\mu_j)^2\ , \tag{B12}$$

we have

$$\begin{aligned} a&=m(1,2)\ ,\\ b&=\mu_0 m(1,2)+\mu_1 m(2,0)+\mu_2 m(0,1)-4\mu_0\mu_1\mu_2\ ,\\ c&=m(0,1)m(2,0)\ . \end{aligned} \tag{B13}$$

Note that we have made a variable transformation $t=cv$. The contour ξ_v is $(0,\infty)e^{i\phi_v}$, with

$$\phi_v=\arg\left[\frac{\mu_2}{m(0,1)m(1,2)}\right]\ . \tag{B14}$$

In arriving at Eq. (B11), we assumed that $\mathrm{Re}(\mu_i)>0$ for $i=0,1,2$. However, we can analytically continue the integral on the right-hand side of Eq. (B11) to $\mathrm{Re}(\mu_i)<0$ provided that a path can be chosen such that, as μ_i is varied from $\mathrm{Re}(\mu_i)>0$ to $\mathrm{Re}(\mu_i)<0$, no singularity of the integrand crosses the contour ξ_v.

By exhausting all permutations of the indices 1, 2, and 3, we find six possible correct contours whose angles are

$$\phi_v=\arg\left[\frac{\mu_0}{m(0,1)m(1,2)},\frac{\mu_0}{m(1,2)m(2,0)},\frac{\mu_1}{m(1,2)m(2,0)},\frac{\mu_1}{m(2,0)m(0,1)},\frac{\mu_2}{m(0,1)m(1,2)},\frac{\mu_2}{m(2,0)m(0,1)}\right]\ . \tag{B15}$$

For a given application, we choose a specific contour, either from the above six contours, or from a combination of them, by noting the property that between any two of the six contours there is no singularity in the integrand of Eq. (B11).

Finally, by a variable transformation $v=s/c$, we obtain

$$I(\mu_0,\mu_1,\mu_2;\mathbf{q}_0,\mathbf{q}_1,\mathbf{q}_2)=2\pi^2\int_{\xi_s}\frac{ds}{as^2+2bs+c}\ , \tag{B16}$$

with the contour ξ_s being $(0,\infty)e^{i\phi_s}$, where

$$\phi_s=\phi_v+\arg[m(0,1)m(2,0)]\ . \tag{B17}$$

If the μ_i's are real and positive, as in Lewis's application, we have $\phi_s=0$, that is, the contour ξ_s is the positive real axis. It is important to note, however, that, in general, a branch point may lie between ξ_s and the positive real axis so that ξ_s cannot be rotated into the positive real axis.

[1] Z.-J. Teng and R. Shakeshaft, Phys. Rev. A **47**, R3487 (1993).
[2] J. A. R. Samson, C. H. Greene, and R. J. Bartlett, Phys. Rev. Lett. **71**, 201 (1993).
[3] L. R. Anderson and J. Burgdörfer, Phys. Rev. Lett. **71**, 50 (1993).
[4] S. L. Carter and H. P. Kelly, Phys. Rev. A **24**, 170 (1981).
[5] M. Ya. Amusia, E. G. Drukarev, V. G. Gorshkov, and M. Kazachkov, J. Phys. B **8**, 1248 (1975).
[6] T. Ishihara, K. Hino, and J. H. McGuire, Phys. Rev. A **44**, R6980 (1991).
[7] T. A. Carlson, Phys. Rev. **156**, 142 (1967).
[8] F. W. Byron and C. J. Joachain, Phys. Rev. **164**, 1 (1967).
[9] T. N. Chang and R. T. Poe, Phys. Rev. A **12**, 1432 (1975).
[10] J. A. R. Samson, Phys. Rev. Lett. **65**, 2861 (1990).
[11] A. Dalgarno and H. R. Sadeghpour, Phys. Rev. A **46**, R3591 (1992).
[12] K. Hino, T. Ishihara, F. Shimizu, N. Toshima, and J. H. McGuire, Phys. Rev. A **48**, 1271 (1993).
[13] T. Åberg, Phys. Rev. A **2**, 1726 (1970).
[14] T. Kato, Commun. Pure. Appl. Math. **10**, 151 (1957).
[15] M. Brauner, J. S. Briggs, and H. Klar, J. Phys. B **22**, 2265 (1989).
[16] C. Garibotti and J. E. Miraglia, Phys. Rev. A **21**, 572 (1980).
[17] C. N. Yang, Phys. Rev. **74**, 764 (1948).
[18] G. H. Wannier, Phys. Rev. **90**, 817 (1953); **100**, 1180 (1955).
[19] A. R. P. Rau, J. Phys. B **9**, L283 (1976).
[20] A. R. P. Feagin, J. Phys. B **17**, 2433 (1984).
[21] However, the use of an angular probability distribution that is Gaussian has been questioned recently. See A. K. Kazansky and V. N. Ostrovsky, Phys. Rev. A **48**, R871 (1993).
[22] F. Maulbetsch and J. S. Briggs, Phys. Rev. Lett. **68**, 2004 (1992).
[23] K. Hino, Phys. Rev. A **47**, 4845 (1993).
[24] Note that an estimate of the contribution of a mechanism depends not only on the gauge but also on the quantitative interpretation of that mechanism. Our interpretation differs from the interpretation based on many-body theory, where each mechanism is fully identified with a particular diagram in the expansion of the ionization amplitude in powers of a potential that s defined as the correlation in the *initial bound* state. See, e.g., Hino *et al.*, Ref. [12].

[25] J. A. R. Samson (private communication).
[26] J. A. R. Samson, R. J. Bartlett, and Z. X. He, Phys. Rev. A **46**, 7277 (1992).
[27] A. Dalgarno and A. L. Stewart, Proc. Phys. Soc., London **76**, 49 (1960).
[28] J. C. Levin, D. W. Lindle, N. Keller, R. D. Miller, Y. Azuma, N. Berrah Mansour, H. G. Berry, and I. A. Sellin, Phys. Rev. Lett. **67**, 968 (1991); J. C. Levin, I. A. Sellin, B. M. Johnson, D. W. Lindle, R. D. Miller, N. Berrah Mansour, Y. Azuma, H. G. Berry, and D. H. Lee, Phys. Rev. A **47**, 16 (1993).
[29] See, e.g., Landau and Lifschitz, *Quantum Mechanics,* 2nd ed. (Pergamon, New York, 1965), p. 524.
[30] R. R. Lewis, Phys. Rev. **102**, 537 (1956).